

## Ferromagnetic resonance studies of NiO-coupled thin films of Ni<sub>80</sub>Fe<sub>20</sub>

R. D. McMichael,\* M. D. Stiles, P. J. Chen, and W. F. Egelhoff, Jr.  
*National Institute of Standards and Technology, Gaithersburg, Maryland 20899*

(Received 23 December 1997)

This paper describes ferromagnetic resonance (FMR) and magnetoresistive measurements of thin magnetic films coupled to antiferromagnetic films. First, FMR results for films of Ni<sub>80</sub>Fe<sub>20</sub> show that coupling to NiO produces the angular variation in the resonance field of the type expected for unidirectional exchange anisotropy. However, unidirectional anisotropy values measured by in-plane ferromagnetic resonance are roughly 20% less than the loop shift measured via magnetoresistance. The difference is attributed in part to asymmetry in the coercivity. Second, in addition to the unidirectional anisotropy, coupling to NiO produces an isotropic negative resonance field shift that is larger than the exchange anisotropy field. This isotropic field shift is not consistent with models of exchange anisotropy in which the ferromagnet spins couple to a static antiferromagnet spin structure. It is consistent with the existence of a rotatable anisotropy, explained in terms of the energetics of domain configurations in the NiO. Third, using unpinned films as references, unidirectional anisotropy is measured for the first time with the magnetization rotated out of the film plane, and is found to be in reasonable agreement with in-plane measurements. [S0163-1829(98)05937-2]

### I. INTRODUCTION

The interaction between ferromagnetic and antiferromagnetic films produces a host of phenomena including hysteresis loop shifts and increased coercivity,<sup>1</sup> training effects,<sup>2</sup> rotational hysteresis at high field,<sup>2</sup> and rotatable anisotropy.<sup>3,4</sup> The related effects observed in ferromagnetic resonance experiments include unidirectional anisotropy, increased resonance linewidth, and ferromagnetic resonance-field (frequency) shifts.<sup>5-7</sup>

Coupled ferromagnetic (F) and antiferromagnetic (AF) films have been studied predominantly through hysteretic measurements of effective exchange bias field  $H_{ex}$  and coercivity  $H_c$ . These measurements yield important information about magnetization reversal, and characterize, in some way, the energy barriers encountered by the magnetization during reversal. It has become common practice to average the zero-crossing fields of a  $M$  vs  $H$  hysteresis loop to obtain a value for  $H_{ex}$ , but this procedure relies on the assumption that the effective coercivities in the ascending and descending parts of hysteresis loop are identical. This assumption is called into question by recent images of domain structures in Ni<sub>80</sub>Fe<sub>20</sub> on single-crystal NiO that indicate that the domain nucleation sites in ascending and descending branches of the hysteresis loop are quite different.<sup>8</sup>

Perturbative measurements, rather than reversing the magnetization, move the magnetization only a small amount during the measurement. Perturbative measurements are complementary to hysteresis measurements in that they characterize the free energy of the system in the neighborhoods of energy minima. Examples of perturbative measurements in F/AF systems include ferromagnetic resonance (FMR) measurements of Ni<sub>80</sub>Fe<sub>20</sub> coupled to FeMn,<sup>5,7,9,10</sup> Brillouin light scattering (BLS),<sup>11</sup> anisotropic magnetoresistance (AMR) measurements of small-angle perturbations,<sup>12</sup> and ac susceptibility of oxidized Co films.<sup>13</sup>

From a theoretical standpoint, perturbative measurements are expected to be more accessible than hysteretic measure-

ments. On a microscopic level, models of perturbative measurements of exchange anisotropy involve calculation of an effective free energy of the ferromagnetic film and its derivatives. In contrast, complete models of hysteretic measurements would also require prediction of magnetization reversal mechanisms and coercivity, which is a significantly more challenging task.

Proposed models for coupling between ferromagnets and antiferromagnets fall into two classes. In one class, the antiferromagnet spin configuration is fixed when  $\mathbf{M}$  is rotated. In these models, the exchange anisotropy is due to the exchange coupling between the ferromagnet spins and uncompensated antiferromagnet spins, which remain essentially frozen in place as  $\mathbf{M}$  is rotated. In some of these models, the ferromagnet spins couple to an average net  $\sqrt{N}$  spins in independent regions of  $N$  interfacial spins.<sup>14,15</sup> The size of an independent region is modeled as the grain size,<sup>15</sup> or as a minimum antiferromagnet domain size.<sup>14</sup> These models yield correct order-of-magnitude results for  $H_{ex}$ .

In another class of models, the antiferromagnet spin configuration changes when  $\mathbf{M}$  is rotated. The coupling at the interface in these models is strong, either because the interface is assumed to be uncompensated,<sup>16</sup> or because the spins on a compensated interface are allowed to cant, giving perpendicular coupling.<sup>17</sup> When  $\mathbf{M}$  is rotated, a partial domain wall is formed that lies parallel to the interface in the antiferromagnet.<sup>16-18</sup> The exchange anisotropy is due to the energy of the domain wall that winds and unwinds as  $\mathbf{M}$  is rotated. These models also yield a correct order of magnitude for  $H_{ex}$ .

Because both of the above classes of models yield correct order-of-magnitude results for  $H_{ex}$ , they are difficult to distinguish through measurements of  $H_{ex}$  alone. This paper describes ferromagnetic resonance and magnetoresistance measurements of thin films of Ni<sub>80</sub>Fe<sub>20</sub> on NiO. FMR and magnetoresistance measurements of  $H_{ex}$  are compared, both for in-plane and out-of-plane rotation of  $\mathbf{M}$ , and the resonance field shift is used to indicate the presence of movable

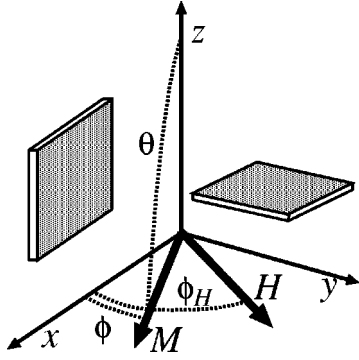


FIG. 1. The coordinate system used in the ferromagnetic resonance measurements.  $\mathbf{H}$  lies in the  $x$ - $y$  plane. Sample orientations for out-of-plane (left) and in-plane (right) measurements are indicated.

antiferromagnetic spin configurations. Section II contains a phenomenological model for the ferromagnetic resonance of films with exchange anisotropy that will be used to interpret the experimental results. The experiments are described in Sec. III. In Sec. III A, differences between hysteretic and perturbative measurements of  $H_{\text{ex}}$  are presented and attributed, in part, to asymmetry of the hysteresis loop. The existence of an isotropic resonance field shift in NiO-coupled films is presented in Sec. III B, and in Sec. III C experiments are described for the first time that measure  $H_{\text{ex}}$  with  $\mathbf{M}$  oriented perpendicular to the film.

## II. MODEL

In ferromagnetic resonance, the precession of a magnetic moment with free energy  $\mathcal{F}(\theta, \phi)$  occurs at a frequency given by

$$\left(\frac{\omega}{\gamma}\right)^2 = \frac{1}{M^2 \sin^2(\theta)} \left[ \frac{\partial^2 \mathcal{F}}{\partial \theta^2} \frac{\partial^2 \mathcal{F}}{\partial \phi^2} - \left( \frac{\partial^2 \mathcal{F}}{\partial \theta \partial \phi} \right)^2 \right], \quad (1)$$

where the partial derivatives are evaluated at values of  $\theta$  and  $\phi$  (see Fig. 1) that minimize  $\mathcal{F}$ , and  $\gamma$  is the gyromagnetic ratio. Note that the resonance frequency is related to the second derivatives of  $\mathcal{F}$ , and is essentially a measure of the ‘‘curvature’’ of  $\mathcal{F}$ , or of the ‘‘stiffness’’ of  $\mathbf{M}$ . In the experiments described below, the magnetization is perturbed at a constant pumping frequency  $\omega_p$  and  $\mathcal{F}$  is modified by varying an applied field. The field needed to modify  $\mathcal{F}$  such that  $\omega = \omega_p$  is referred to as the resonance field  $H_{\text{res}}$ .

In the data to be presented below, comparisons will be made between the resonance fields for films coupled to NiO and resonance fields for uncoupled, control films. Because coupling to NiO is expected to modify  $\mathcal{F}$ , it is useful to consider the effect on the resonance fields when a small energy term is added to  $\mathcal{F}$ . If the magnetization is oriented along a minimum, or ‘‘easy’’ direction of the added energy, the curvature of  $\mathcal{F}$  is increased, and the applied field needed to make the resonance frequency equal to the pumping frequency  $H_{\text{res}}$  is decreased. Similarly, if the magnetization is oriented along a hard direction of the additional energy,  $H_{\text{res}}$  is increased. An increased value of  $H_{\text{res}}$  corresponds to a hard direction and a decreased value of  $H_{\text{res}}$  corresponds to an easy direction.

We model the free energy  $\mathcal{F}$  of the magnetization of a ferromagnetic film coupled to an antiferromagnet as the sum of the free energy of the uncoupled ferromagnetic film  $\mathcal{F}_0$  and a contribution due to coupling to the antiferromagnet  $\mathcal{F}_{\text{AF}}$

$$\mathcal{F} = \mathcal{F}_0 + \mathcal{F}_{\text{AF}}, \quad (2)$$

$$\begin{aligned} \mathcal{F} = & K_u (\hat{\mathbf{m}} \cdot \hat{\mathbf{n}})^2 + K_a (\hat{\mathbf{m}} \cdot \hat{\mathbf{p}})^2 - \mu_0 \mathbf{M} \cdot \mathbf{H}_0 \\ & - \mu_0 \mathbf{M} \cdot \mathbf{H}_{\text{ex}} - \mu_0 \mathbf{M} \cdot \mathbf{H}_{\text{ra}}. \end{aligned} \quad (3)$$

The first two terms represent uniaxial anisotropies, one with a hard axis along  $\hat{\mathbf{n}}$ , the film normal, and one with a hard axis along  $\hat{\mathbf{p}}$ , a unit vector in the plane of the film, and  $\hat{\mathbf{m}} = \mathbf{M}/M$  is the direction of the magnetization. The corresponding anisotropy fields are  $H_u = 2K_u/\mu_0 M$  and  $H_a = 2K_a/\mu_0 M$ , respectively.  $K_u$  includes the magnetostatic shape anisotropy energy  $(\mu_0/2)M^2$  ( $2\pi M^2$  in cgs units). The third term represents the interaction of the magnetization with an applied field  $\mathbf{H}_0$ .

The last two terms in Eq. (3) represent  $\mathcal{F}_{\text{AF}}$ . The term involving  $\mathbf{H}_{\text{ex}}$  is the unidirectional exchange anisotropy energy which, depending on the model, is either the energy required to reversibly form domain walls or spirals in the antiferromagnet as the magnetization is rotated through macroscopic angles,<sup>16–18</sup> or the energy of the exchange coupling of the ferromagnet to uncompensated spins on the antiferromagnet interface.<sup>14,15</sup> The exchange anisotropy field  $\mathbf{H}_{\text{ex}}$  is fixed when the biased state is established. Similar terms have appeared in previous analyses of FMR results in films with exchange anisotropy.<sup>5,7,9,10</sup>

The last term in Eq. (3) is introduced here to model the isotropic resonance field shifts that will be described in Sec. III B. The rotatable anisotropy field<sup>3,4</sup>  $\mathbf{H}_{\text{ra}}$  is a field that rotates to be roughly parallel to  $\hat{\mathbf{m}}_0$ , the steady-state value of  $\hat{\mathbf{m}}$  that minimizes  $\mathcal{F}$ . This term includes some of the effects of domain-wall hysteresis in the antiferromagnet<sup>18</sup> into a model appropriate for interpretation of perturbative measurements such as FMR, BLS, small-angle AMR, and ac susceptibility.

As a possible mechanism for an effective rotatable anisotropy, consider the situation when a ferromagnetic film is coupled to a domain structure in the antiferromagnet that changes *irreversibly* as the ferromagnet  $\hat{\mathbf{m}}$  is rotated through large angles. During any macroscopic rotation of  $\hat{\mathbf{m}}$ , some part of the AF domain structure will relax to a local energy minimum state, establishing a new direction for  $\hat{\mathbf{m}}_0$ . Subsequent small rotations of  $\hat{\mathbf{m}}$  away from the new  $\hat{\mathbf{m}}_0$  will reversibly perturb the antiferromagnetic domain structure in the neighborhood of its energy minimum. Because these perturbations will tend to raise the energy of the system, a stiffening torque will tend to return  $\hat{\mathbf{m}}$  toward its steady-state orientation as the antiferromagnetic domain structure returns to its local equilibrium state. We model this torque as an effective field  $\mathbf{H}_{\text{ra}}$  that is parallel to  $\hat{\mathbf{m}}_0$ . In a sense, the antiferromagnet domain structure in this example provides a

‘rotatable anisotropy’ with an easy direction that follows the macroscopic motion of  $\hat{\mathbf{m}}_0$ , decreasing  $H_{\text{res}}$  in all directions.

Note that including  $\mathbf{H}_{\text{ra}}$  in Eq. (3) does not reproduce an actual rotational hysteresis, since it exerts no torque on  $\mathbf{M}_0$ . The term including  $\mathbf{H}_{\text{ra}}$  only describes an effect on perturbative measurements that is consistent with rotational hysteresis. A more detailed model of rotational hysteresis requires a description of antiferromagnet domain configuration.<sup>18</sup>

Also note that in models where exchange anisotropy effects are solely due to interfacial exchange interactions with a fixed antiferromagnet spin configuration, there is no hysteretic motion of antiferromagnet domain walls. The effect of the interface on the ferromagnet is simply a Zeeman-like, single-valued, surface-energy term of the type modeled by  $\mathbf{H}_{\text{ex}}$ . Models having static antiferromagnetic spin configurations do not predict an isotropic resonance-field shift of the type modeled by  $\mathbf{H}_{\text{ra}}$ .

### III. EXPERIMENT

The samples were prepared by dc magnetron sputtering in 26 mPa (2 mTorr) of Ar. The base pressure before depositing a film was typically  $10^{-6}$  Pa ( $10^{-8}$  Torr) of which 90% of the residual gas is hydrogen. Permanent magnets adjacent to the substrate holder provide a field that determines the direction of the exchange anisotropy field during deposition. To measure resonance-field shifts and increases in linewidth due to coupling between thin ferromagnetic films and NiO, measurements were made on pairs of films: one of each pair with the ferromagnetic film deposited directly on NiO and the other, ‘control,’ film with the ferromagnetic film separated from the NiO. The films were capped with 5.0 nm of Au or Ta to protect against oxidation.

In two of the pairs described in this paper, one with 5-nm-thick  $\text{Ni}_{80}\text{Fe}_{20}$  films and the other with 10-nm-thick  $\text{Ni}_{80}\text{Fe}_{20}$  films, each film of the pair films was deposited separately, one on NiO and the other on NiO covered by 2 nm Ta. The 10-nm control film was found to have a 9.4-mT uniaxial in-plane anisotropy field that we attribute to off-axis sputtering of Ta. The sputtering gun was located approximately  $45^\circ$  from the film normal, and the easy direction is perpendicular to the Ta atom flux. For the 5-nm control film, the substrate was rotated  $90^\circ$  after the first 5 nm of Ta were deposited, and the anisotropy field was reduced to 1.2 mT. Similar magnetic films deposited on glass without Ta show much smaller in-plane anisotropy.

Magneto-resistive measurements and thermal treatments to reset the exchange anisotropy field were carried out in a separate apparatus with a vacuum estimated to be better than 1 mPa ( $10^{-5}$  Torr). The sample was mounted inside a temperature-controlled copper enclosure, where four-wire magneto-resistance measurements were made. Electrical contacts to the samples were made using spring-loaded pins in a nominally square configuration with the voltage and current contacts arranged approximately parallel to the field direction. On a microscopic level, the resistivity  $\rho$  of the films can be described by

$$\rho = \rho_0 + \Delta\rho \cos^2(\theta_{\mathbf{J},\mathbf{M}}), \quad (4)$$

where  $\Delta\rho$  is the anisotropic magnetoresistance and  $\theta_{\mathbf{J},\mathbf{M}}$  is the angle between the current density  $\mathbf{J}$  and the magnetization,  $\mathbf{M}$ . As the field is reversed,  $\mathbf{M}$  deviates from the direction of  $\mathbf{J}$  (and  $\mathbf{H}$ ) and the measured resistance  $R$  passes through a minimum. We use the average of the minimum  $R$  fields in the descending and ascending branches of the hysteresis loop to determine  $H_{\text{ex}}$ . This method differs from common practice, which is to use the average of the  $M=0$  (coercive) fields to determine  $H_{\text{ex}}$ . However, there is no reason, in principle, why fields of maximum transverse moment, maximum susceptibility, or even maximum time dependence could not be used to determine  $H_{\text{ex}}$ . All these possible measurements share the assumption of symmetry of the hysteresis loops about  $H_{\text{ex}}$  and all would be expected to yield identical values if the loop is symmetric.

In other experiments, the film pairs were combined in single samples to ensure that the films had identical orientations with respect to the applied field. These samples have a spin-valve-like structure<sup>19</sup> with one film deposited on NiO, and the ‘control’ film separated from the pinned film by 5.0 nm Cu.

The ferromagnetic resonance measurements were made at 9.77 GHz, with the sample mounted on a goniometer having vernier scale with  $\pm 0.15^\circ$  resolution. Alignment of the sample was achieved by rotating it about two orthogonal directions to maximize the free film resonance field at perpendicular resonance. Using this method, a conservative estimate is that it is possible to align the sample to within  $\pm 0.1^\circ$ .

Temperature variation in the FMR apparatus was accomplished through the use of a triple-walled quartz cavity insert that allowed flow of heated  $\text{N}_2$  gas over the sample. To minimize temperature differences between the sample and the inlet to the cavity, where the temperature was monitored, gas passing over the sample is redirected to pass between the first (innermost) and second walls of the insert, heating the wall nearest the sample. The space between the second and third (outermost) walls is evacuated. In addition, a high flow rate of approximately 500 l/h of  $\text{N}_2$  was used, and the incident microwave power was kept low (0.2 mW) to avoid additional heating of the sample.

#### A. Comparison of hysteretic and perturbative measurements

In this section, ferromagnetic resonance measurements and magnetoresistive hysteresis measurements of  $H_{\text{ex}}$  are compared as a function of temperature. The sample consists of 5.0 nm  $\text{Ni}_{80}\text{Fe}_{20}$  on 50 nm NiO with a 6.0-nm cap layer of Ta. In the FMR experiments, resonance spectra at each temperature were recorded with the applied field oriented parallel and antiparallel to the orientation of the field that was applied during sample deposition. Magneto-resistance measurements were made on a separate piece of the same sample at sequentially higher temperatures. The results are plotted in Fig. 2. The  $H_{\text{ex}}$  values appear to decrease linearly, becoming insignificant at a blocking temperature of  $\approx 200^\circ\text{C}$ . It is also clear from these results that  $H_{\text{ex}}$  measured through hysteresis is about 20% larger than  $H_{\text{ex}}$  measured by resonance.

This difference was larger in a sample consisting of 10.0 nm  $\text{Ni}_{80}\text{Fe}_{20}$  on NiO with a 10-nm cap of Au. After field cooling from  $235^\circ\text{C}$ , the magneto-resistance measurement in this sample gave  $H_{\text{ex}} = 6.5$  mT. For the FMR measurements,

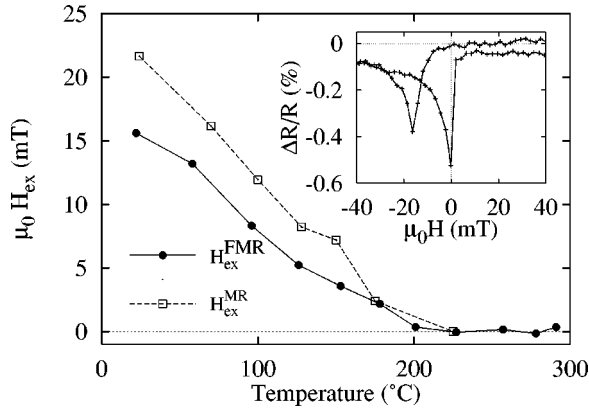


FIG. 2. Unidirectional anisotropy field as a function of temperature for a 5-nm film of  $\text{Ni}_{80}\text{Fe}_{20}$  on NiO measured by ferromagnetic resonance and by magnetoresistance measurements of magnetization reversal. Inset: magnetoresistance at 128 °C showing asymmetry of the hysteresis loop.

the film was oriented in the  $x$ - $y$  plane of the coordinate system in Fig. 1. The resonance-field data, shown in Fig. 3, were fit using the model in Eq. (3) using a weighted orthogonal distance regression algorithm.<sup>20</sup> The fit yields  $\mu_0 H_{ex} = 2.0 \pm 0.1$  mT, which is less than a third of the magnetoresistance value. The fit also yields an anisotropy field of  $\mu_0 H_a = 1.9 \pm 0.1$  mT for the NiO-coupled film. The upper curve in Fig. 3 shows the resonance fields of the 10-nm  $\text{Ni}_{80}\text{Fe}_{20}$  control film deposited on Ta. The angular variation of the resonance field in the control film is dominated by a  $9.4 \pm 0.1$ -mT in-plane anisotropy that is attributed to off-axis sputtering of Ta as described above.

A difference of 30% between hysteretic and FMR measurements of  $H_{ex}$  has been noted for  $\text{Ni}_{80}\text{Fe}_{20}$  coupled to FeMn, although in this case the difference was attributed to

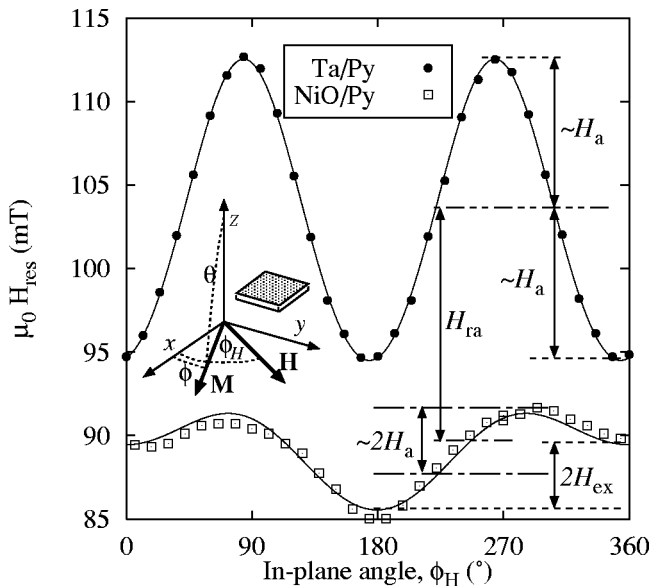


FIG. 3. In-plane resonance fields for 10-nm films of  $\text{Ni}_{80}\text{Fe}_{20}$  on NiO (NiO/Py) and a control film separated from NiO by 2 nm Ta (Ta/Py). The solid lines are fits to the data yielding an in-plane anisotropy field of 9.4 mT for the control film and  $\mu_0 H_{ex} = 2.0$  mT,  $\mu_0 H_a = 1.9$  mT for the NiO-coupled film.

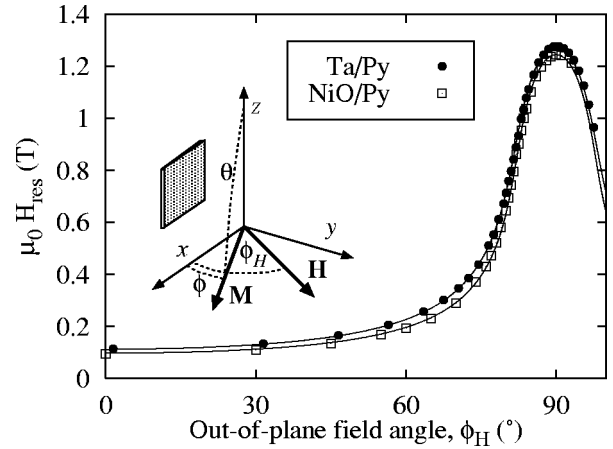


FIG. 4. Out-of-plane resonance fields for a 10-nm  $\text{Ni}_{80}\text{Fe}_{20}$  film deposited on NiO (NiO/Py) and for a 10-nm  $\text{Ni}_{80}\text{Fe}_{20}$  film separated from NiO by 20 nm of Ta (Ta/Py). The solid lines are fits to the data.

sample heating through microwave absorption.<sup>6</sup> We have ruled out sample heating as a major contribution to the difference between our hysteretic and FMR measurements through FMR spectra taken as a function of microwave power. Using the temperature-dependent field shift, which is discussed below in Sec. III B, as an internal sample thermometer, we found that the temperature at our working power level of 0.2 mW was identical to the extrapolated zero-power results to within experimental uncertainty.

The difference between the FMR and hysteretic values of  $H_{ex}$  may be attributable to asymmetry in the hysteresis loop. Note that the AMR loop displayed in the inset of Fig. 2 is asymmetric, having different minimum resistance values in the ascending and descending branches of the hysteresis loop, and slower saturation in negative fields than in positive fields. Asymmetry is also prominent in the hysteresis loop of the 10-nm  $\text{Ni}_{80}\text{Fe}_{20}$  sample described above. Such asymmetry is an indication that extracting a value of  $H_{ex}$  from the average of the minimum resistance fields is not strictly valid in these samples. The asymmetry of the hysteresis loop would also affect the validity of values of  $H_{ex}$  extracted from the hysteresis loop by any other hysteretic method.

## B. Resonance-field shifts

In this section, resonance fields of NiO-coupled films and control films are compared as a function of applied-field orientation and temperature to measure the properties of  $\mathbf{H}_{ra}$ .

In Fig. 4, resonance fields are plotted for a pair of films with 10-nm-thick  $\text{Ni}_{80}\text{Fe}_{20}$  layers capped by 10 nm Au. Referring to the coordinate system in Fig. 1, the films were oriented in the  $x$ - $z$  plane with  $\mathbf{H}_{ex}$  directed along the  $z$  axis. In this orientation,  $\mathbf{M}$  is very nearly perpendicular to  $\mathbf{H}_{ex}$  and the effects of  $\mathbf{H}_{ex}$  are minimized since the second derivatives of  $-\mathbf{M} \cdot \mathbf{H}_{ex}$  in Eq. (1) are nearly zero. Resonance fields (not shown) were also measured with  $\mathbf{H}_{ex}$  directed along the  $x$  axis. In all orientations, the resonance field of the pinned film was found to be lower than that of the control film.

The existence of an isotropic resonance-field shift is significant because it is not predicted by previous models. Pre-

TABLE I. Results of least-squares fitting to resonance field data in Fig. 4 for 10-nm films of  $\text{Ni}_{80}\text{Fe}_{20}$  on NiO and on Ta. Parentheses indicate values that were held fixed during the fit. Indicated uncertainties are the greater of the standard deviations of the fit or the uncertainty in resonance-field measurements.

	NiO\Ta\Py	NiO\Py
$\omega/\gamma$ (mT)	$330.1 \pm 0.5$	(330.1) <sup>a</sup>
$g$	$2.11 \pm 0.01$	(2.11) <sup>a</sup>
$\mu_0 H_u$ (mT)	$941.1 \pm 0.5$	$924.2 \pm 1.0$
$\mu_0 H_a$ (mT)	(9.4) <sup>b</sup>	(1.9) <sup>b</sup>
$\mu_0 H_{ra}$ (mT)	(0)	$10.1 \pm 0.03$

<sup>a</sup>Value determined by fit to control film data.

<sup>b</sup>Value determined by fit to in-plane data.

vious models of the field shift,<sup>6,7,21</sup> based on measurements made with the magnetization lying in plane,<sup>6,7,11</sup> have identified the shift as a surface anisotropy. These models predict negative field shifts when the magnetization is directed along an easy direction, or in an easy plane of the surface anisotropy. However, these models also predict positive field shifts when the magnetization is directed along the hard direction of the surface anisotropy. The data presented in Figs. 3 and 4, for both in-plane and out-of-plane directed resonance, cannot be modeled by an anisotropy with static easy and hard axes.

The existence of an isotropic resonance field shift has further significance because it is an indicator that the coupling with the antiferromagnet makes a contribution  $\mathcal{F}_{AF}(\theta, \phi)$  to the free energy of the ferromagnetic film that is not a continuous, single valued, doubly differentiable function of  $\theta$  and  $\phi$ . As described in the previous paragraph, a single-valued doubly differentiable function would have maxima and minima with negative and positive curvature that would increase or decrease the resonance field, respectively, depending on the magnetization direction. On the other hand, an isotropic negative field shift is possible if  $\mathcal{F}_{AF}(\theta, \phi)$  is multivalued or not differentiable in a way such that the maxima (negative curvature regions) are not accessible. For example, a multivalued energy function that is not stable in the regions near the energy maxima may switch hysteretically to lower energy, higher curvature sheets. Examples of multivalued energy terms can be found in Refs. 17 and 18. The term in Eq. (3) that includes  $\mathbf{H}_{ra}$  is also a multivalued function of  $\theta$  and  $\phi$  that takes on different values for each orientation of the steady-state magnetization direction  $\hat{\mathbf{m}}_0$ . Alternatively, the interaction energy function may be single valued, but with cusps at the maxima such that the magnetization is not stable at the cusp where the curvature (loosely defined) is negative.

The resonance fields plotted in Fig. 4 were fit to a free energy of the form given by Eq. (3), incorporating values of  $H_a$  determined from the in-plane resonances described in the previous subsection. The fit results, which were used to generate the curves in Fig. 4, are given in Table I. The results for the NiO-coupled film include a rotatable anisotropy field value of  $\mu_0 H_{ra} = 10.1$  mT. The field shift  $H_{ra}$  is larger than the exchange anisotropy field values determined by magnetoresistance (6.5 mT) or by FMR (2.0 mT) on the same sample.

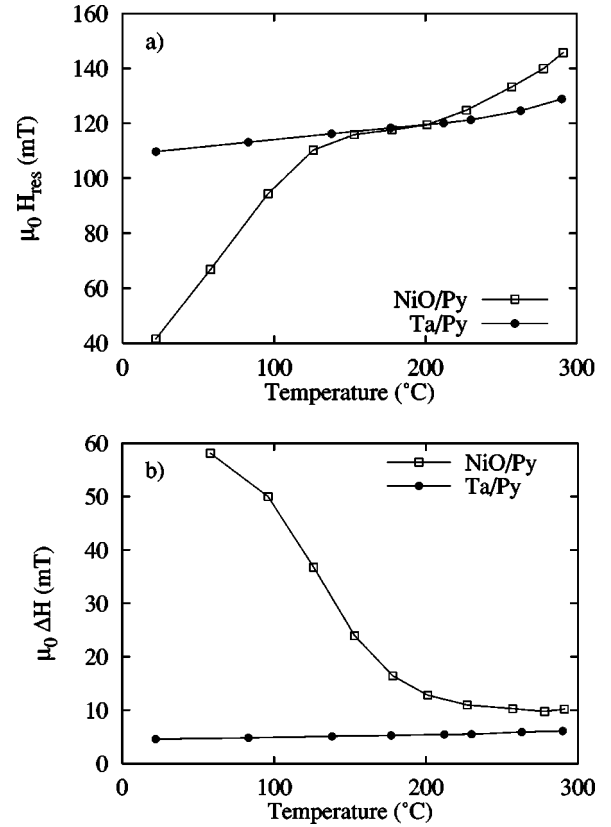


FIG. 5. (a) In-plane resonance fields and (b) linewidth of 5.0-nm films of  $\text{Ni}_{80}\text{Fe}_{20}$  deposited on NiO (NiO/Py) and on Ta (Ta/Py) as a function of temperature.

An alternate fit to the  $\text{Ni}_{80}\text{Fe}_{20}$  on NiO data was also obtained without using a rotatable anisotropy term. This fit yields  $\omega/\gamma = 311.8$  mT, or  $g = 2.24$ . We reject this alternate fit result for two reasons. First, in-plane FMR in this sample at 35.0 GHz occurs at 800 mT, in agreement with  $g = 2.10$ , where  $g = 2.24$  would predict resonance at 750 mT. Second, in NiFe/FeMn bilayers and sandwiches, Stoecklein *et al.* have shown that  $g$  does not depend on NiFe thickness.<sup>7</sup> A thickness dependence would be expected if there was an interfacial effect on  $g$  due to coupling with the antiferromagnetic FeMn.

The temperature dependence of the in-plane resonance fields and linewidths were measured on a pair of 5.0-nm  $\text{Ni}_{80}\text{Fe}_{20}$  films on NiO and Ta. See Fig. 5. For the NiO-coupled film, the plotted value of  $H_{res}$  is the average of the two resonance fields measured with the applied field directed opposite and along  $\mathbf{H}_{ex}$ . The  $H_{res}$  values for the control film were taken with the applied field along the in-plane easy axis. The in-plane anisotropy field in the control film is 1.2 mT at room temperature. We attribute the increases in  $H_{res}$  above 200 °C to irreversible changes in the films. In terms of the energy model proposed above, the difference between the resonance fields of the NiO-coupled and control films is the rotatable anisotropy field  $H_{ra}$  plus corrections due to the small differences between the uniaxial in-plane and out-of-plane anisotropy fields of the two films. It appears that  $H_{ra}$  becomes insignificant at a temperature near 125 °C. In contrast, the linewidth [see Fig. 5(b)] and exchange anisotropy field (see Fig. 2) become insignificant at a higher temperature near 200 °C.

### C. Measurements near perpendicular resonance

In this section, values of  $\mathbf{H}_{\text{ex}}$  from measurements made with  $\mathbf{M}$  in plane are compared with values of  $\mathbf{H}_{\text{ex}}$  made with  $\mathbf{M}$  oriented near the film normal.

In many samples of interest, where the antiferromagnet-coupled film is strongly pinned, measurement of exchange bias by in-plane FMR can be difficult. The increased linewidth reduces the amplitude of the resonance, and the field shift moves the resonance toward zero field where the magnetization may not be saturated. If a higher FMR frequency is used, the resonance will occur at higher field, but the line will be further broadened. In spin valves,<sup>19</sup> for which there is a great deal of technical interest,<sup>22</sup> FMR measurements of the antiferromagnet-pinned film are further complicated by the presence of a strong resonance from the free film that tends to swamp the signal from the pinned film.

Near perpendicular resonance, however, the linewidth of a pinned film is strongly reduced.<sup>23</sup> In addition, the resonance field is a sensitive function of field orientation, peaking sharply when the magnetization is held perpendicular to the plane of the film. These conditions make it possible to measure  $H_{\text{ex}}$  with the magnetization directed out of plane by a method described below.

Because the uniaxial anisotropy  $K_u$ , which includes magnetostatic shape effects, is by far the dominant energy term in the free energy of the magnetization in these samples [see Eq. (3)], the maximum resonance field  $H_{\text{res}}^{\text{max}}$  will be found when  $\mathbf{M}$  is perpendicular to the film. Referring to Fig. 1, if the film is placed in the  $x$ - $z$  plane with  $\mathbf{H}_{\text{ex}}$  directed along the  $x$  axis, the magnetization will have an equilibrium orientation perpendicular to the film only if the applied field contains a component with magnitude  $H_{\text{ex}}$  directed along the  $-x$  axis. The  $y$  component of the applied field can be adjusted to satisfy the resonance condition (1). The resulting resonance field will be at an angle  $\delta\phi = \sin^{-1}(H_{\text{ex}}/H_{\text{res}}^{\text{max}})$  from the film normal.

Because  $H_{\text{ex}}$  (order mT) is much smaller than  $H_{\text{res}}^{\text{max}}$  (order T) we expect  $\delta\phi$  to be small. To precisely determine the film normal, we used a spin-valve-like sample incorporating both a NiO-coupled  $\text{Ni}_{80}\text{Fe}_{20}$  film and a free film. The structure of the sample is  $\text{Si}\backslash 50 \text{ nm NiO}\backslash 5 \text{ nm Ni}_{80}\text{Fe}_{20}\backslash 5 \text{ nm Cu}\backslash 5 \text{ nm Ni}_{80}\text{Fe}_{20}\backslash 5 \text{ nm Ta}$ . One  $\text{Ni}_{80}\text{Fe}_{20}$  layer, sandwiched between Cu and Ta, is “free,” and serves as a control film. The other  $\text{Ni}_{80}\text{Fe}_{20}$  test layer is “pinned” by its interactions with the antiferromagnetic NiO layer. The maximum resonance field of the control film serves as a precise indicator of the sample orientation and eliminates the need to independently align the films in the goniometer with high precision. In addition, the structure exhibits giant magnetoresistance, which allows an independent resistive measurement of the exchange anisotropy field.

The ability of the free film to indicate the sample orientation is not expected to depend on differences in film stress, composition, or microstructure that may exist between the free and pinned films. The free film may be slightly affected by coupling to the pinned film, but this is expected to be a very minor effect since the free and pinned film moments are very nearly parallel, and since the coupling is an order of magnitude smaller than  $H_{\text{ex}}$ .

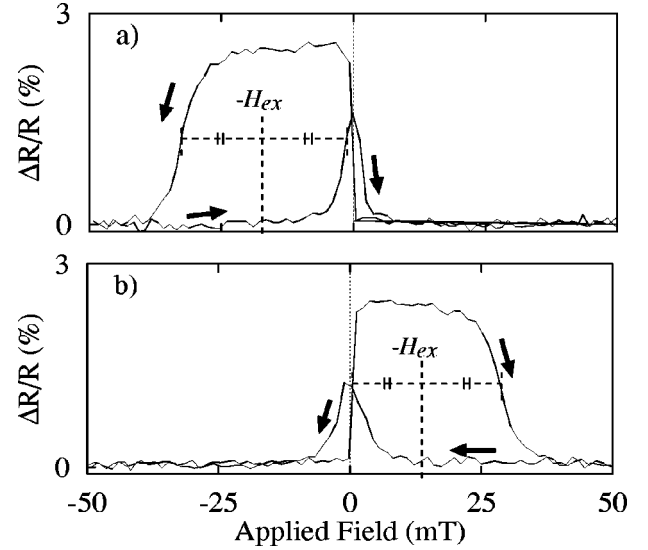


FIG. 6. Magnetoresistance curves measured after (a) setting and (b) reversing the exchange anisotropy field direction. The curves illustrate the method of determining  $H_{\text{ex}}$  and show the nearly complete reversal of  $H_{\text{ex}}$  achieved by the “set” and “reverse” processes.

The exchange anisotropy direction was “set” by heating the sample to 200 °C in vacuum for 1 min, and cooling slowly to room temperature in a field directed parallel to the field that was applied during deposition. After magnetoresistive and FMR measurements were made, the bias direction was “reversed” by again heating to 200 °C for 1 min, and cooling in an oppositely directed field. The magnetoresistive and FMR measurements were then repeated. Magnetoresistance curves are plotted in Fig. 6.

Minor loop magnetoresistance curves measured in low field (not shown) indicate that the free film is nearly completely aligned with the applied field for applied field magnitudes  $> \sim 1$  mT. Because giant magnetoresistance depends on the relative orientation of the magnetization (GMR) of the free and pinned layers, the resistance of the sample effectively measures the alignment of the pinned film with the applied field, except in low fields ( $< \sim 1$  mT). Using the half-maximum points in Fig. 6,  $H_{\text{ex}}$  is determined to be 16.0 mT after setting  $\mathbf{H}_{\text{ex}}$ , and after reversal  $H_{\text{ex}} = 13.6$  mT. Minor loops (not shown) indicate that the coupling between the  $\text{Ni}_{80}\text{Fe}_{20}$  layers is less than 0.2 mT in both cases. The result that  $H_{\text{ex}}$  is smaller after reversal may be due to irreversible changes such as those observed in the temperature-dependence experiments at temperatures above 200 °C, or, because the temperature was raised only to 200 °C, and not to the ordering temperature of NiO, near 250 °C, the exchange anisotropy may not be completely reversed in the setting/reversing procedure.

Resonance fields measured near perpendicular resonance before and after resetting the bias direction are plotted in Fig. 7. To determine the angle of maximum resonance field  $\phi_{\text{max}}$  for each film, the data in the interval  $85^\circ \leq \phi \leq 95^\circ$  were fit to a function of the form  $H_{\text{res}}(\phi) = a - b(\phi - \phi_{\text{max}})^2 - c(\phi - \phi_{\text{max}})^4$ . The difference between the fit values of  $\phi_{\text{max}}$  for the free and pinned films in each case is taken to be a measurement of  $\delta\phi$ . The values of  $\delta\phi$  and their corresponding values of  $H_{\text{ex}}$  are presented in Table II with values of

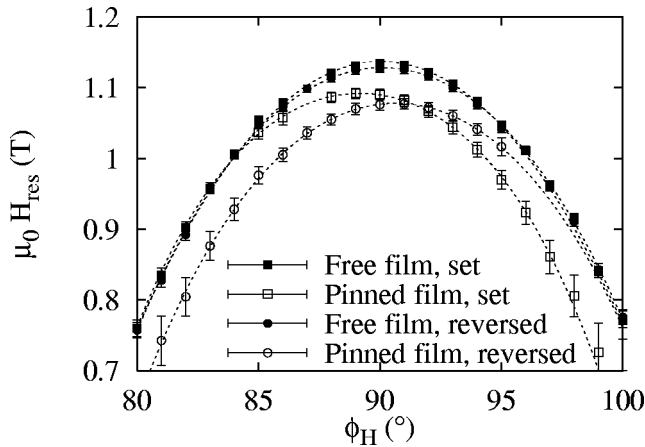


FIG. 7. FMR fields measured near perpendicular orientation of the NiO/Ni<sub>80</sub>Fe<sub>20</sub>/Cu/Ni<sub>80</sub>Fe<sub>20</sub>/Ta film. In the set direction,  $\mathbf{H}_{\text{ex}} \parallel \mathbf{H}_{\text{app}}$  at  $\phi_H = 180^\circ$ , and in the reverse direction  $\mathbf{H}_{\text{ex}} \parallel \mathbf{H}_{\text{app}}$  at  $\phi_H = 0^\circ$ . Dotted lines are quartic fits to the data for  $85^\circ \leq \phi_H \leq 95^\circ$ , and the error bars indicate the peak-to-peak linewidth of the resonances.

$H_{\text{ex}}$  from the GMR measurements. The agreement between the FMR and GMR values for  $H_{\text{ex}}$  is quite good, especially considering the fact that FMR and magnetoresistive measurements described above in Sec. III A differ by approximately 20%. This agreement is consistent with a lack of strong texture in the polycrystalline NiO.

#### IV. SUMMARY

The experiments described in this paper lead to three major results. First, there is an isotropic FMR field shift, characterized by a rotatable anisotropy field  $H_{\text{ra}}$ ; in NiO-biased films, it is larger than angular variation due to the bias field  $H_{\text{ex}}$ . This result is consistent with a rotatable anisotropy having an easy axis that follows the equilibrium orientation of the magnetization for macroscopic changes of  $\mathbf{M}$  but that can be regarded as stationary for perturbations of  $\mathbf{M}$ . The observed isotropic resonance-field shift is consistent with coupling to a hysteretic system such as a domain structure in the antiferromagnetic NiO. The isotropic field shift is not consistent with models of exchange anisotropy in which the

TABLE II. Values of  $\delta\phi$  and  $H_{\text{ex}}$  determined from the angular dependence of FMR data and  $H_{\text{ex}}$  from GMR measurements.

	$\delta\phi$	$H_{\text{ex}}$ , FMR (mT)	$H_{\text{ex}}$ , GMR (mT)
Set	$0.88 \pm 0.03^\circ$	$16.5 \pm 0.6$	16.5
Reversed	$-0.56 \pm 0.02^\circ$	$-10.5 \pm 0.4$	-13.6

ferromagnet couples to a static antiferromagnet spin configuration.

Second, the value of  $H_{\text{ex}}$  determined by FMR is close to, but consistently less than, the value determined through hysteresis measurements. Asymmetry in the measured magnetoresistance curves suggests that at least part of this difference may be due to asymmetric magnetization reversal mechanisms giving different values of coercivity for the descending and ascending parts of the hysteresis loop, so that the “true” value of  $H_{\text{ex}}$  is not exactly halfway between the  $M = 0$  points.

Miller *et al.* report a perturbative measurement made on oxidized Co using magnetoresistance as a probe of the magnetization response to a small applied field, in which the perturbative measurement yields a *higher* value of  $H_{\text{ex}}$  than a hysteresis measurement.<sup>12</sup> However, in Ref. 12 the magnetic response to the perturbations is evaluated only with  $\mathbf{M}$  aligned with  $\mathbf{H}_{\text{ex}}$ , and the results are interpreted in terms of a model that did not include a rotatable anisotropy field such as  $\mathbf{H}_{\text{ra}}$ . In terms of the phenomenological model used in this paper, values of  $H_{\text{ex}}$  from Refs. 12 and 13 would be reinterpreted as  $H_{\text{ex}} + H_{\text{ra}}$ .

Third, for polycrystalline NiO, comparable values of  $H_{\text{ex}}$  are obtained for  $\mathbf{M}$  in the plane of the sample, and for  $\mathbf{M}$  rotated out of the plane. This last result may not hold for single-crystal antiferromagnets. In fact, comparisons of in-plane and out-of-plane measurements of  $H_{\text{ex}}$  can be expected to yield information about the symmetry of the interfacial coupling in single-crystal or highly textured films.

#### ACKNOWLEDGMENTS

The authors thank J. J. Krebs for assistance with Q-band FMR measurements and R. V. Drew and H. J. Brown for technical assistance.

\*Electronic address: rmc michael@nist.gov

<sup>1</sup>W. H. Meiklejohn and C. P. Bean, Phys. Rev. **102**, 1413 (1956).

<sup>2</sup>C. Schlenker, J. Phys. (Paris), Colloq. **2**, 157 (1968).

<sup>3</sup>R. J. Prosen, J. O. Holmen, and B. E. Gran, J. Appl. Phys. **32**, 91S (1961).

<sup>4</sup>J. M. Lommel and C. D. Graham, Jr., J. Appl. Phys. **33**, 1160 (1962).

<sup>5</sup>J. C. Scott, J. Appl. Phys. **57**, 3681 (1985).

<sup>6</sup>V. S. Speriosu, S. S. P. Parkin, and C. H. Wilts, IEEE Trans. Magn. **23**, 2999 (1987).

<sup>7</sup>W. Stoecklein, S. S. P. Parkin, and J. C. Scott, Phys. Rev. B **38**, 6847 (1988).

<sup>8</sup>V. I. Nikitenko, V. S. Gornakov, L. M. Dedukh, Yu. P. Kabanov, A. F. Khapikov, A. J. Shapiro, R. D. Shull, A. Chaiken, and R. P. Michel, Phys. Rev. B **57**, R8111 (1998).

<sup>9</sup>A. Layadi, W. C. Cain, J.-W. Lee, and J. O. Artman, IEEE Trans. Magn. **23**, 2993 (1987).

<sup>10</sup>R. D. McMichael, W. F. Egelhoff, Jr., and L. H. Bennett, IEEE Trans. Magn. **31**, 3930 (1995).

<sup>11</sup>A. Ercole, T. Fujimoto, M. Patel, C. Daboo, R. J. Hicken, and J. A. C. Bland, J. Magn. Mater. **156**, 121 (1996).

<sup>12</sup>B. H. Miller and E. Dan Dahlberg, Appl. Phys. Lett. **69**, 3932 (1996).

<sup>13</sup>Valter Ström, B. J. Jönsson, K. V. Rao, and Dan Dahlberg, J. Appl. Phys. **81**, 5003 (1997).

<sup>14</sup>A. P. Malozemoff, Phys. Rev. B **35**, 3679 (1987); J. Appl. Phys. **63**, 3874 (1988).

<sup>15</sup>Kentaro Takano, R. H. Kodama, A. E. Berkowitz, W. Cao, and G. Thomas, Phys. Rev. Lett. **79**, 1130 (1997).

<sup>16</sup>D. Mauri, H. C. Siegmann, P. S. Bagus, and E. Kay, J. Appl. Phys. **62**, 3047 (1987).

<sup>17</sup>N. C. Koon, Phys. Rev. Lett. **78**, 4865 (1997).

<sup>18</sup>M. D. Stiles and R. D. McMichael (unpublished).

- <sup>19</sup>B. Dieny, V. S. Speriosu, S. S. P. Parkin, B. A. Gurney, D. R. Wilhoit, and D. Mauri, *Phys. Rev. B* **43**, 1297 (1991); see also E. Velu, C. Dupas, D. Renard, J. P. Renard, and J. Seiden, *ibid.* **37**, 668 (1988); G. Binasch, P. Grunberg, F. S. Saurenbach, and W. Zinn, *ibid.* **39**, 4828 (1994).
- <sup>20</sup>P. T. Boggs and J. E. Rogers, *Contemp. Math.* **112**, 183 (1990).
- <sup>21</sup>R. L. Stamps, R. E. Camley, and R. J. Hicken, *Phys. Rev. B* **54**, 4159 (1996).
- <sup>22</sup>J. A. Brug, L. Tran, M. Bhattacharyya, J. H. Nickel, T. C. Anthony, and A. Jander, *J. Appl. Phys.* **79**, 4491 (1996).
- <sup>23</sup>R. D. McMichael, M. D. Stiles, P. J. Chen, and W. F. Egelhoff, Jr., *J. Appl. Phys.* **83**, 7037 (1998).